

RESEARCH ARTICLE

Open Access



Transcriptome analysis reveals self-incompatibility in the tea plant (*Camellia sinensis*) might be under gametophytic control

Cheng-Cai Zhang^{1,2†}, Li-Yuan Wang^{1†}, Kang Wei¹, Li-Yun Wu¹, Hai-Lin Li¹, Fen Zhang¹, Hao Cheng^{1*} and De-Jiang Ni^{2*}

Abstract

Background: Self-incompatibility (SI) is under genetic control and prevents inbreeding depression in angiosperms. SI mechanisms are quite complicated and still poorly understood in many plants. Tea (*Camellia sinensis* L.) belonging to the family of Theaceae, exhibits high levels of SI and high heterozygosity. Uncovering the molecular basis of SI of the tea plant may enhance breeding and simplify genomics research for the whole family.

Results: The growth of pollen tubes following selfing and crossing was observed using fluorescence microscopy. Self-pollen tubes grew slower than cross treatments from 24 h to 72 h after pollination. RNA-seq was employed to explore the molecular mechanisms of SI and to identify SI-related genes in *C. sinensis*. Self and cross-pollinated styles were collected at 24 h, 48 h and 72 h after pollination. Six RNA-seq libraries (SP24, SP48, SP72, CP24 CP48 and CP72; SP = self-pollinated, CP = cross-pollinated) were constructed and separately sequenced. In total, 299.327 million raw reads were generated. Following assembly, 63,762 unigenes were identified, and 27,264 (42.76 %) unigenes were annotated in five public databases: NR, KOG, KEGG, Swiss-Port and GO. To identify SI-related genes, the fragments per kb per million mapped reads (FPKM) values of each unigene were evaluated. Comparisons of CP24 vs. SP24, CP48 vs. SP48 and CP72 vs. SP72 revealed differential expression of 3,182, 3,575 and 3,709 genes, respectively. Consequently, several ubiquitin-mediated proteolysis, Ca²⁺ signaling, apoptosis and defense-associated genes were obtained. The temporal expression pattern of genes following CP and SP was analyzed; 6 peroxidase, 1 polyphenol oxidase and 7 salicylic acid biosynthetic process-related genes were identified. The RNA-seq data were validated by qRT-PCR of 15 unigenes. Finally, a unigene (CL25983Contig1) with strong homology to the S-RNase was analyzed. It was mainly expressed in styles, with dramatically higher expression in self-pollinated versus cross-pollinated tissues at 24 h post-pollination.

Conclusions: The present study reports the transcriptome of styles after cross- and self-pollination in tea and offers novel insights into the molecular mechanism behind SI in *C. sinensis*. We believe that this RNA-seq dataset will be useful for improvement in *C. sinensis* as well as other plants in the Theaceae family.

Keywords: *Camellia sinensis*, Theaceae, Tea, Transcriptome, Self-incompatibility, S-RNase, Gametophytic

* Correspondence: chenghao@tricaas.com; nidj@mail.hzau.edu.cn

†Equal contributors

¹Key Laboratory of Tea Biology and Resources Utilization, Ministry of Agriculture, Tea Research Institute Chinese Academy of Agricultural Sciences, 9 Meiling South Road, Hangzhou 310008, China

²College of Horticulture and Forestry Science, Huazhong Agricultural University, No.1, Shizishan Street, Hongshan District, Wuhan, Hubei Province 430070, China



Background

Self-incompatibility (SI) is genetically controlled, and promotes outcrossing while preventing inbreeding depression in flowering plants [1]. Although SI has emerged as a model for cell-cell communication and signal transduction [2, 3], it is also an agriculturally important trait [4, 5]. Although SI has been widely demonstrated in angiosperms, its mechanism has been elucidated in only a few plants [6]. Sporophytic SI (SSI) in Brassicaceae is controlled by the stigma-specific S-receptor kinase (SRK) and pollen-specific S-locus cysteine-rich protein (SCR), which inhibits germination and growth of self-pollen on the stigma [7]. While during gametophytic SI (GSI) in *Rosaceae*, *Solanaceae* and *Plantaginaceae*, the interaction between the female determinant S-RNase and the male component S-locus F-box protein (SLF/SFB) mediate the rejection response of self-pollen tubes in the pistil [8–10]. Another GSI mechanism exists in *Papaveraceae* in which a Ca^{2+} signaling cascade leads to programmed cell death (PCD) [11]. Additionally, many species demonstrate SI from pollen inhibition in the ovary, which is called either ovarian SI (OSI) or late-acting SI (LSI). This form of SI was defined according to the location of the pollen inhibition instead of the genetic mechanism of SI as with GSI and SSI [12]. LSI is more widespread among the basal groups of Angiosperms, which indicates a conserved ancestral mechanism of SI; nevertheless, its molecular basis still remains unclear [6, 13]. Some types of LSI may be controlled by either the gametophyte or sporophyte independently, whereas other types may be jointly controlled [13].

Overall, SI is regulated by multiple genes and associated with different metabolic pathways. Next Generation Sequencing (NGS) and transcriptome analysis has revealed candidate genes that contribute to SI interaction in *Citrus clementine* [14], *Citrus limon* [4] and *Leymus chinensis* [3].

The Theaceae family consists of 20 genera and over 600 species [15]. Several of the species in these subclasses have significant economic value, such as Tea (*C. sinensis* L.), Tea-oil tree (*C. oleifera* Abel.) and the ornamental Sasanqua (*C. sasanqua* Thunb.). Due to their self-incompatibility, Theaceae species are highly heterogeneous, making crop improvement via classical breeding and genetics difficult [16], it and has hindered genetic map construction and contig assembly from whole-genome sequencing [16–18]. Therefore, uncovering the molecular basis of SI in Theaceae may simplify and enhance breeding and genomics in this family.

Tea is one of the most prominent beverages in the world [16] and is widespread in tropical and subtropical regions [15]. It is also a model for studying SI [19, 20]. Tea has exhibited GSI because of a self-pollen tube growth inhibiting at the base of the style [21, 22]. However, more recent evidence suggests LSI because the pollen tubes from self-

fertilized flowers were inhibited in the ovary [23, 24]. Similarly, the edible oil plant of *C. oleifera* also manifests LSI behavior [5]. In these studies, although pollen tubes from self-pollinations penetrated the ovary, pollen tube growth was inhibited to some extent in the style. In contrast, pollen tubes from cross-pollination reached the ovary with no interference [5, 22–24]. Therefore, the differential growth of the pollen tube from self and cross-pollinations was a critical trait in understanding SI in *C. sinensis*.

Attempts have been made to understand the molecular mechanisms underlying tea SI [16, 21, 25]. A pistil-specific pathogenesis-related-1 (PR-1) protein was identified in tea, but the relationship between PR-1 and SI was not clearly demonstrated [21]. cDNA-AFLP method was also used to analyze differentially expressed genes in self-incompatible lines of tea, and 34 genes were isolated which were involved in energy metabolism, signal transduction and defense [26]. A *C. sinensis* floral transcriptome analysis revealed the presence of several pollen/pistil specific expression unigenes [16]. The objective of this study was to gain deeper insights into the molecular basis of SI and to provide a global view of candidate SI-related genes in tea using RNA-seq. We believe that the identification of candidate SI-related genes will contribute to a more complete understanding of the SI mechanism in *C. sinensis*, which will improve breeding and genomics research in the Theaceae.

Results and discussion

Observation of pollen tube growth

Pollens from both the cross- and self-pollination germinated at 6 h post-pollination, and no visible differences were observed in pollen tube growth from 6 h to 12 h. At 24 h after pollination, a small number of tubes from the cross-pollination reached the style base (Fig. 1). However, pollen tubes from self-pollination grew more slowly, reaching just the middle of the style. At 48 h after pollination, most tubes from cross-pollination reached the style base, but the pollen tubes from the self-pollination took 72 h to reach the same place. Self-pollen tubes grew slower than cross-pollen tubes from 24 h to 72 h after pollination. This is consistent with previous studies that also showed reduced pollen tube growth from a SI cross [5, 21–23]. The delay in pollen tube growth may be critical for the SI reaction because, by the time that the self-pollen tubes penetrate the ovary, the pistil may have already been primed for abscission [6].

RNA-seq and transcriptome assembly

To uncover the mechanism behind SI reaction in *C. sinensis*, six RNA-seq libraries (CP24, CP48, CP72, SP24, SP48 and SP72) were separately constructed and sequenced. In total, 299.327 million raw reads with a Q30 over 83 % were generated. After removing the low quality sequences

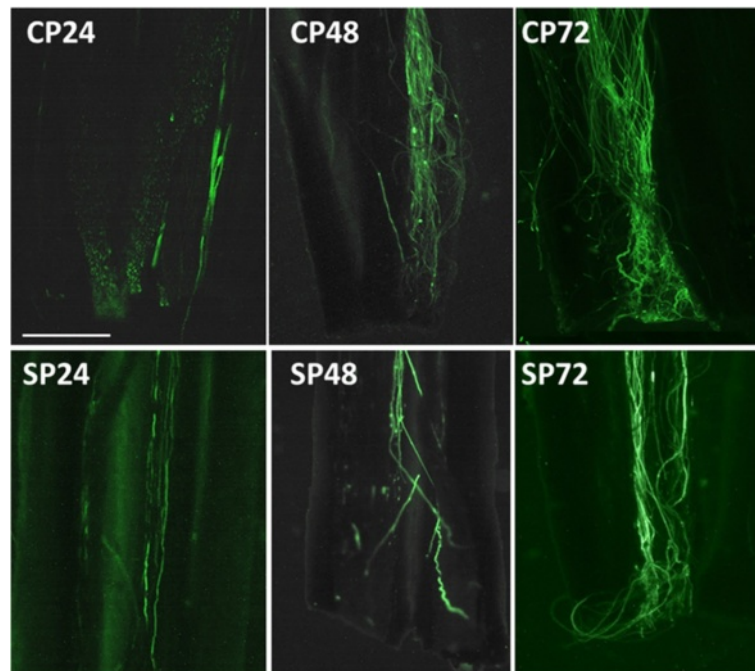


Fig. 1 Pollen tubes growth after CP and SP in *C. sinensis*. CP24: a few pollen tubes reached the style base; CP48 and CP72: a larger number of pollen tubes arrived the style base; SP24: pollen tubes in the middle of the style; SP48: a few pollen tubes reached the style base; SP72: a large number of pollen tubes arrived the style base. Bar = 500 μ m

(length < 35 bp, Q < 20), a total of 294.144 million clean reads were retained (Table 1). After *de novo* assembly using Trinity software, 63,762 unigenes were identified. The lengths of unigenes ranged from 301 bp to 14,580 bp, with an average of 1,018.26 bp and a N50 length of 1,354 bp (Table 2).

Functional annotation

To predict potential functions of the assembled unigenes, all of them were blastx (E-value $\leq 10^{-5}$) against 5 public databases, including the National Center for Biotechnology Information (NCBI) Non-redundant Protein (NR), Clusters of Orthologous Groups for Eukaryotic Complete Genomes (KOG), Kyoto Encyclopedia of Genes

and Genomes (KEGG), Swiss-Prot Protein Database (Swiss-Port) and Gene Ontology (GO) (Fig. 2). Most unigenes (26,984, 42.32 %) were annotated to the NR database, and 16,210 (60.08 %) sequences had significant homology (blastx E-value < 10^{-45}). Among the annotated unigenes, 37 % (9975) and 9.76 % (2631) had strong homology to *Vitis vinifera* and *Theobroma cacao*, respectively (Additional file 1).

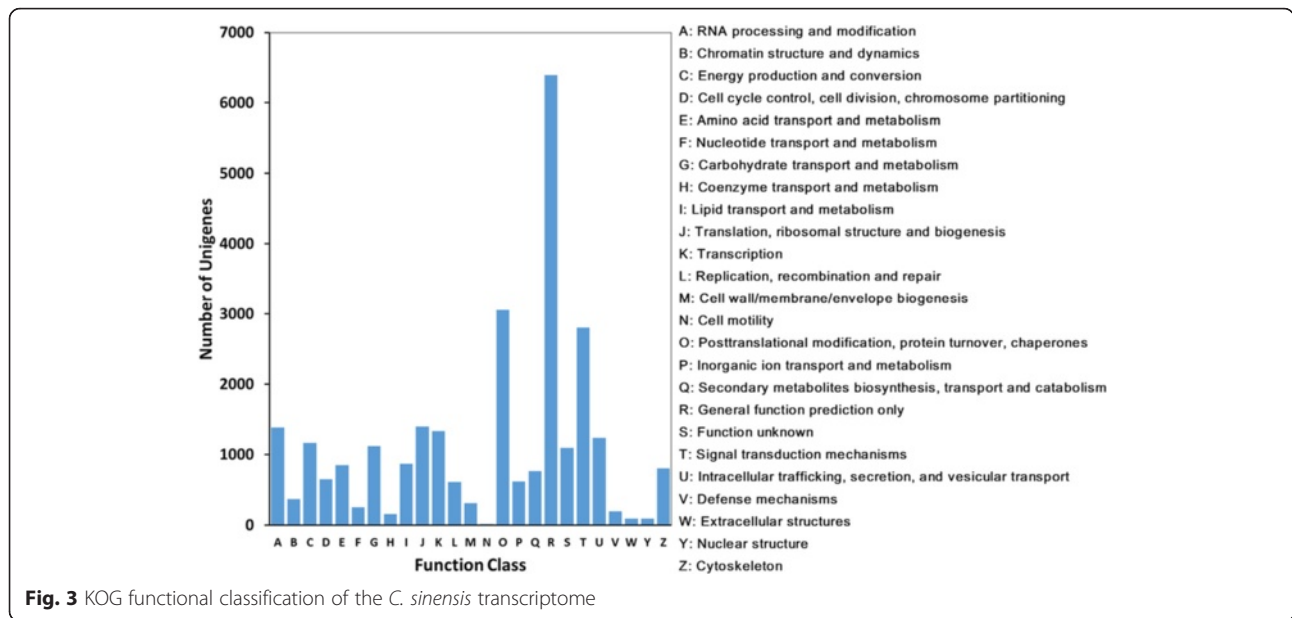
The unigenes were further annotated and classified using the KOG database (Fig. 3). A total of 27,618 unigenes were assigned KOG classifications. Among the 25 KOG categories, the “general function prediction only” (6391, 23.15 %) was the most abundant, followed by “post-translational modification, protein turnover, chaperones” (3054, 11.06 %), “signal transduction mechanisms” (2,803, 10.15 %) and “translation, ribosomal structure and biogenesis” (1394, 5.05 %).

The unigenes were then matched to the GO terms (Additional file 2). A total of 21,932 unigenes were classified into 58 sub-categories belonging to 3 categories (biological process, cellular component and molecular function). Among the biological process category, “metabolic process” and “cellular process” were the main functional groups, which were followed by “single organism process” and “response to stimulus”. In terms of cellular component, “cell part” and “cell” were the most highly represented subcategories. For the molecular function

Table 1 Summary for the RNA-seq outcomes of six separately pooled samples

Sample	CP24 ^a	CP48	CP72	SP24	SP48	SP72	Total
Raw reads (million)	43.798	55.519	54.843	48.094	49.118	47.956	299.327
Clean reads (million)	43.075	54.536	53.905	47.337	48.283	47.008	294.144
Total base (Gb)	5.007	6.339	6.266	5.502	5.612	5.464	34.189
Q30	83.3 %	83.4 %	83.5 %	83.3 %	83.1 %	83.1 %	—

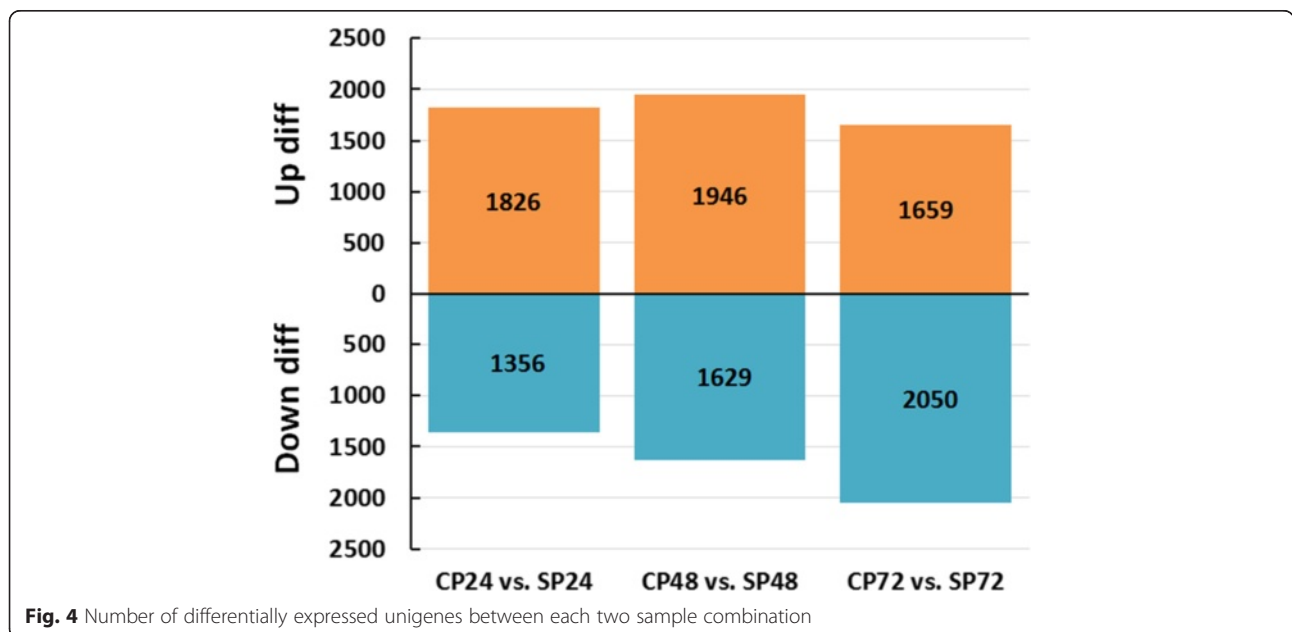
^aCP = cross pollination, SP = self pollination, numbers after CP and SP indicate hours after pollination



between groups of CP24 vs. SP24, CP48 vs. SP48 and CP72 vs. SP72, respectively (Fig. 4, Additional file 3). To determine the putative functions of these genes, GO and KEGG analyses were implemented. Between the group comparing CP24 vs. SP24, 1826 genes were up-regulated and 1356 genes were down-regulated. Among these differentially expressed genes, 1008 were associated with GO categories, and 272 were mapped to 232 KEGG pathways. Similarly, between the group of CP48 vs. SP48, 1946 genes were up-regulated and 1629 genes were down-regulated; 1501 of them were associated with GO categories, and 566 were mapped to 251 KEGG pathways. In

addition, between the group of CP72 vs. SP72, 1659 genes were up-regulated and 2050 genes were down-regulated; 1465 of them were associated with GO categories, and 485 were mapped to 266 KEGG pathways. The high number of differentially expressed unigenes provided an abundant list of candidate SI-related genes. In contrast, cDNA-AFLP analysis of self-incompatible lines of tea previously yielded only 100 polymorphic bands [26]. Therefore, RNA-seq seems to be more productive than cDNA-AFLP for identifying potential SI related genes.

In the above comparisons, some pathways occurred in all three comparisons, such as “phenylpropanoid



biosynthesis”, “phenylalanine metabolism” and “plant-pathogen interaction”. In addition, “ubiquitin mediated proteolysis” [34–36], “apoptosis” [37, 38], “calcium signaling pathway” [30] and several defense-related pathways [3, 39] were also identified as up-regulated pathways that are associated with the SI reaction in plants. Therefore, the unigenes associated with the above pathways may also be associated with SI interaction in tea.

For “ubiquitin mediated proteolysis”, a SCF complex plays a key role in the S-RNase-based GSI system [1, 40]. S-phase kinase-associated protein 1 (Skp-1), F-box, RING-box protein 1 (Rbx1) and Cullin-1 (CUL1) also function as components of the SCF complex [33]. The SCF complex uniquely mediates the ubiquitination of non-self S-RNase, which is then degraded by the 26 s proteasome [33]. In this study, 7 differentially expressed unigenes annotated as *Skp-1* (CL1Contig5289 and CL18002Contig1), *F-box* (CL1Contig1120 and CL1Contig2140), *Rbx1* (CL1Contig679) and *CUL1* (CL1Contig1054 and comp136094_c0_seq6) were identified. These unigenes might be directly related to SI in tea, which warrant further exploration.

Calcium (Ca^{2+}) is a second messenger, which plays a key role in pollen germination and tube growth and serves an important function in the prevention of self-fertilization [30]. Several Ca^{2+} signaling-related genes were identified that may function during SI. Calcium-dependent protein kinase (CDPK) is a Ca^{2+} response element, which localized at the tip of the pollen tube. In *Petunia*,

overexpression the Pi *CDPK1* and the Pi *CDPK2* will disrupt growth polarity or inhibit extension of the pollen tube, respectively [41]. Five predicted *CDPKs* (CL1Contig1101, CL1Contig1911, comp91595_c0_seq1, CL41260Contig1 and comp128850_c0_seq1) were detected; the latter three have higher expression levels in SP samples than CP, which might affect the growth polarity or inhibit the extension of the pollen tubes from self-pollination. The protein families of calmodulin (CaM), calmodulin-like (CML), and calcineurin B-like (CBL) act as sensors during Ca^{2+} signal transduction. Several members of them are expressed pollen-specifically and highly expressed during pollen tube germination and elongation [42]. Here, three *CaMs* (CL20031Contig1, comp152366_c1_seq4 and CL2413Contig1), four *CBLs* (CL1Contig702, CL23964Contig1, CL26666Contig1 and comp88134_c0_seq1), and three *CMLs* (CL27939Contig1, CL33074Contig1, and CL39651Contig1) were identified to be differentially expressed. Therefore, the unigenes annotated as *CDPKs*, *CaMs* and *CMLs* merit special attention.

Gene temporal expression patterns of CP and SP

To identify the temporal expression patterns of genes following self-pollination and cross-pollination treatments (Additional file 4), the short time-series expression miner software (STEM) was employed. The unigenes in CP and SP groups were clustered into 8 profiles (Fig. 5).

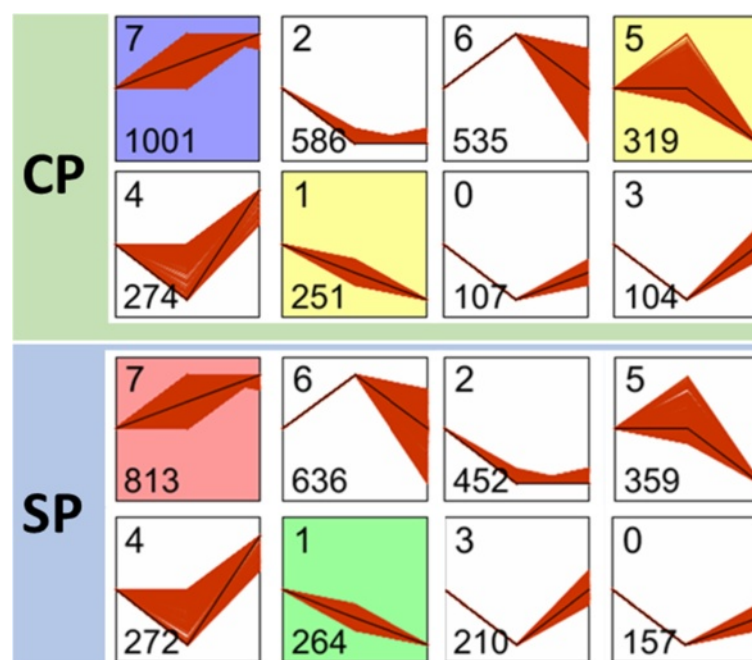


Fig. 5 Different gene expression patterns between CP and SP. Each square represents a pattern. Top number indicates the profile ID number, bottom number indicates the number of time series genes. The patterns were ordered based on the number of genes. The colored squares were significant modules. The horizontal axis represents different times after pollination

Each profile represents a group of genes that exhibited similar expression trend. The highest number of genes in group CP was found in profile 7 (1,001, 31.51 %), followed by profile 2 (586, 18.45 %), profile 6 (535, 16.84 %) and finally profile 5 (319, 10.04 %). While in group SP, profile 7 (813, 25.70 %) was also the largest category, followed by profile 6 (636, 20.11 %), profile 2 (452, 14.29 %) and profile 5 (359, 11.35 %).

Following GO-term analysis to identify the putative functions of genes in profile 7 of both treatments, genes were classified into 3 categories including biological process, cellular component and molecular function (Fig. 6). For the biological process category, “oxidation-reduction process” was the most abundant subcategory in group CP, while 31 genes were classified into “defense response to fungus” (16), “recognition of pollen” (8) and “salicylic acid biosynthetic process” (7) categories. In group SP, “carbohydrate metabolic process” and “response to ethylene” were the dominant groups, while 12 genes were involved in “ethylene-activated signaling pathway” (6) and “cell wall macromolecule catabolic process” (6) subcategories. These results show that cross- and self-pollination result in different gene expression responses in the style.

A total of 83 unigenes were clustered into the “oxidation-reduction process” group, and a heat map was constructed based on the FPKM values of six samples (Fig. 7). Expression of these unigenes steadily increased from 24 h to 72 h in cross-pollinated styles. A similar trend was observed in self-pollinated styles but with a delay. Previous studies have revealed that reactive oxygen species (ROS) regulate stress resistance and pollen tube growth in plants

[43, 44]. ROS concentrations increase in incompatible pollen tubes, leading to deleterious effects and SI-mediated PCD [45]. Various antioxidant systems take part in biological processes to maintain the proper concentration of ROS and prevent the damage from ROS [46]. Here, 6 peroxidases (CL39261Contig1, CL36955Contig1, CL799Contig1, CL31720Contig1, CL1Contig803 and CL13267Contig1), 1 polyphenol oxidase (CL28614Contig1) and several other redox-related genes were greatly increased in cross-pollinated styles, which is consistent with a previous study showing higher activity of peroxidase and polyphenol oxidase in cross-pollinated styles than self-pollinated ones of *C. sinensis* [47]. Among the 6 putative peroxidase genes, 3 unigenes (CL799Contig1, CL39261Contig1 and CL31720Contig1) contained intact ORFs and were homologues to AT5G05340. A multiple sequence alignment of AT5G05340 and the deduced amino acid sequences of CL799Contig1, CL39261Contig1 and CL31720Contig1 were constructed, which share approximately 70 %, 45 % and 41 % identity, respectively (Fig. 8). The gene AT5G05340 encodes a peroxidase (AtPrx 53) enzyme, which is closely related to the cell wall synthesis [48]. Therefore, the higher expression levels of these genes might promote pollen tube elongation during compatible styles.

Furthermore, 7 unigenes (CL1Contig2132, CL1Contig5305, CL20835Contig1, CL25392Contig1, CL29231Contig1, CL35779Contig1 and CL38632Contig1) associated with “salicylic acid biosynthetic process” were also consistently up-regulated in 3 samples of CP. Salicylic acid (SA)

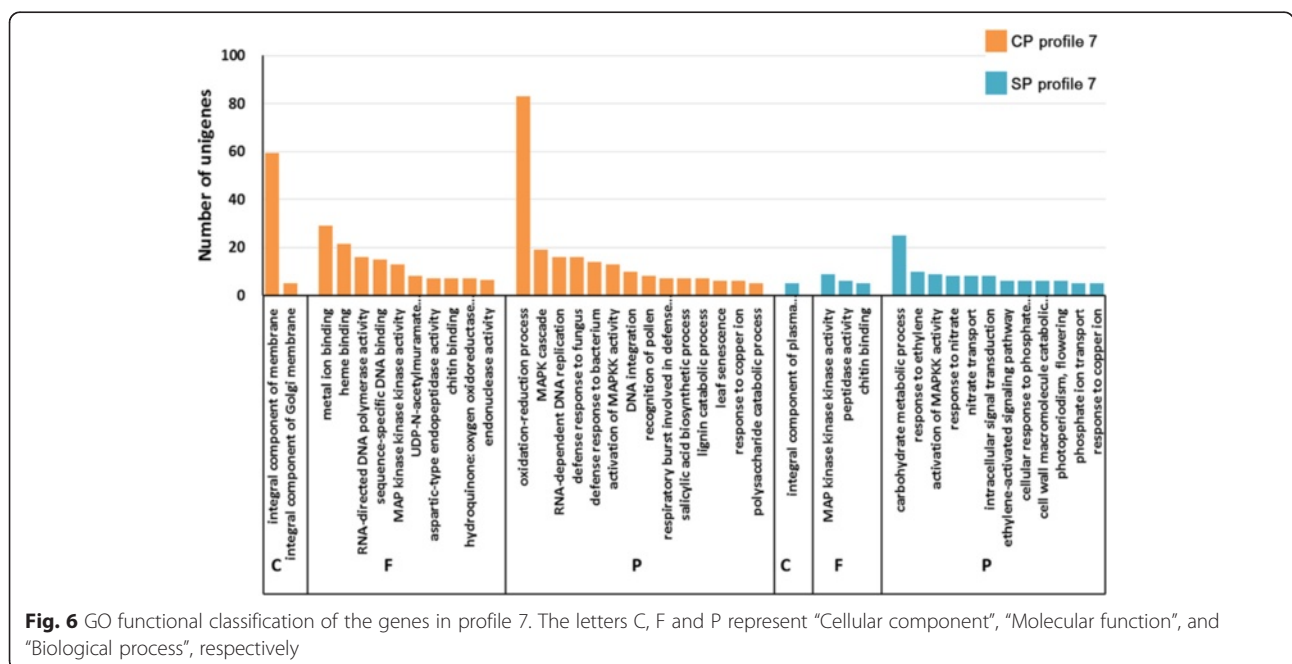


Fig. 6 GO functional classification of the genes in profile 7. The letters C, F and P represent “Cellular component”, “Molecular function”, and “Biological process”, respectively

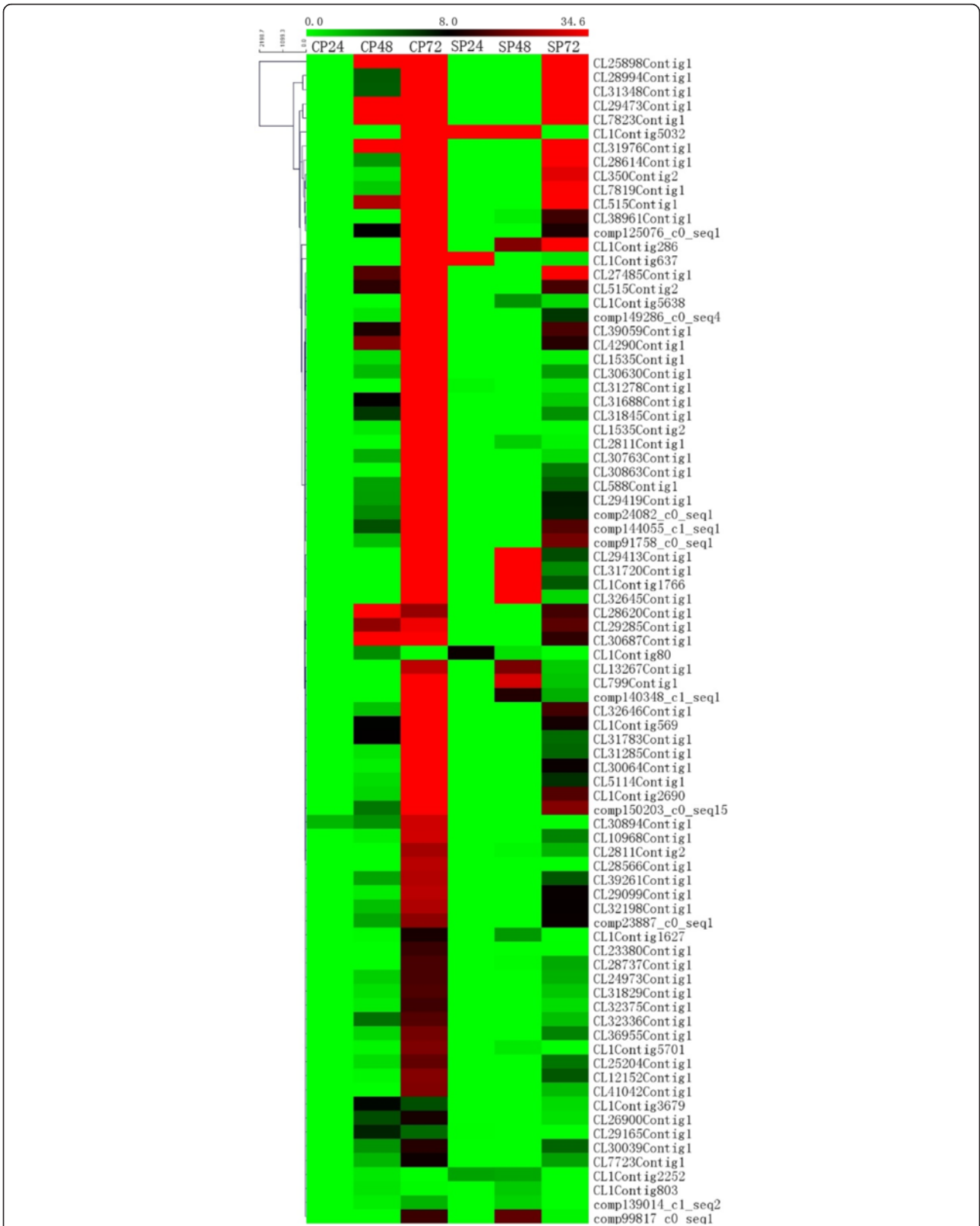


Fig. 7 A heat map of 83 oxidation-reduction process-related unigenes generated using a MeV software. Along the horizontal axis (from left to right): CP24, CP48, CP72, SP24, SP48, SP72. The vertical axis represent the unigenes

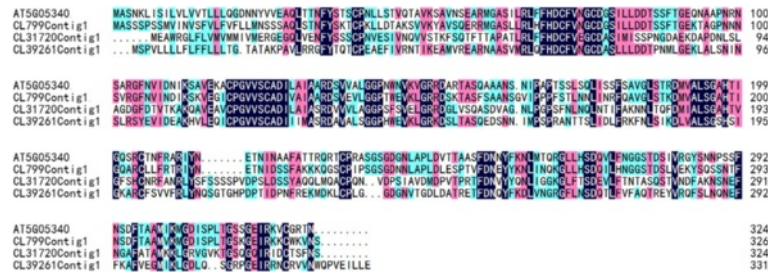


Fig. 8 A multiple alignment of amino acid sequences of AT5G05340, CL799Contig1, CL39261Contig1 and CL31720Contig1 constructed by DNAMAN

may contribute to regulating ROS accumulation [49], and then induce the defense responses and impact the self/non-self recognition as well as the pollen tube growth [50, 51].

Differentially expressed gene validation by qRT-PCR

Fifteen differentially expressed genes were selected to test the reliability of RNA-seq data (Table 3). These genes were associated with “plant-pathogen interaction” (CL1Contig2502, CL25362Contig1, CL25650Contig1, CL21816Contig1 and CL2609Contig1), “flavonoid biosynthesis” (CL32645Contig1, CL28991Contig1 and CL26013Contig1), “ubiquitin mediated proteolysis” (CL1Contig5289 and CL1Contig1054), “apoptosis” (CL12551Contig1),

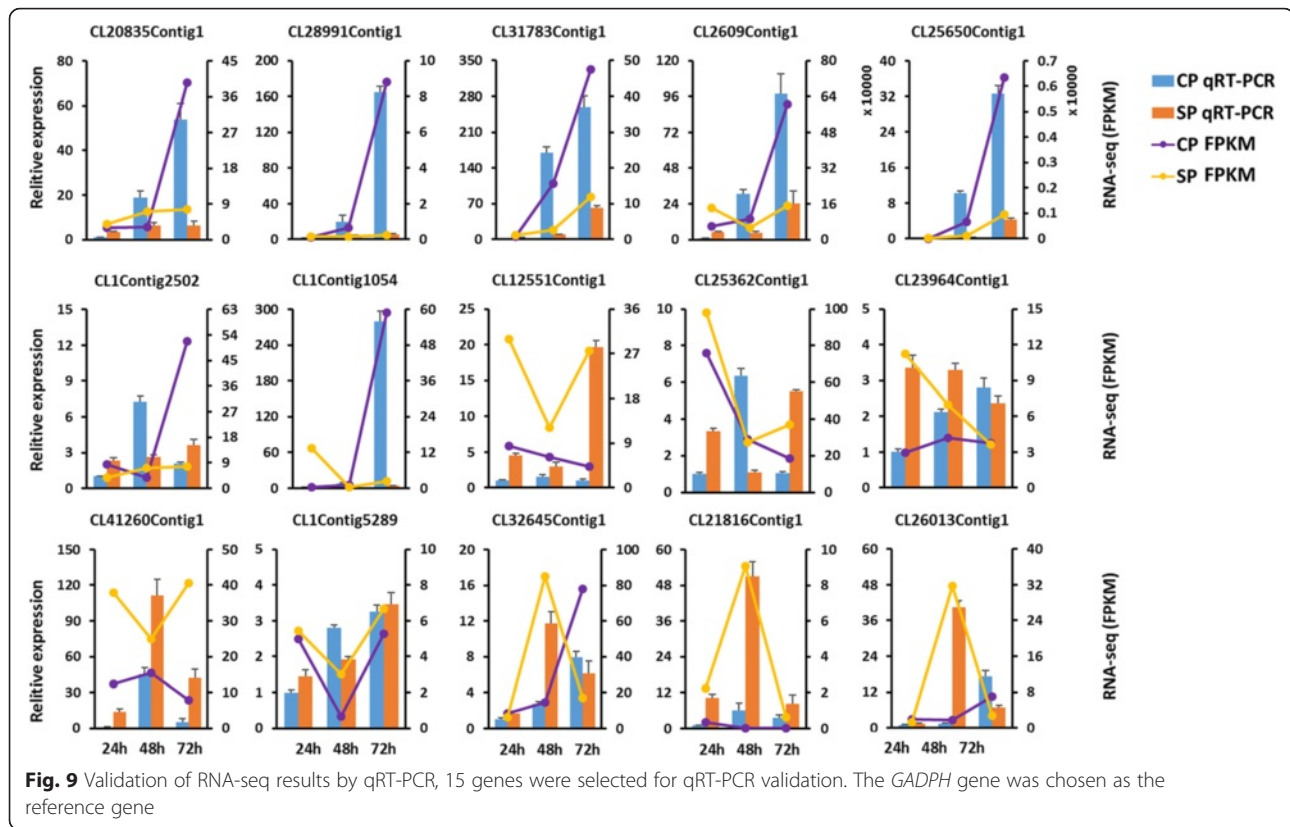
“calcium signaling pathway” (CL23964Contig1), “plant hormone response” (CL25362Contig1 and CL31783Contig1) and “negative regulation of programmed cell death” (CL20835Contig1). The expression patterns for 11 genes (73.3 %) were highly consistent with the sequencing data, while 4 genes (26.7 %, CL1Contig2502, CL25362Contig1, CL25362Contig1 and CL1Contig5289) were partially consistent (Fig. 9). The qRT-PCR results confirmed that the RNA-seq results were relatively accurate.

Analysis of a putative S-RNase gene

S-RNase is associated with GSI in plants of *Rosaceae*, *Solanaceae* and *Plantaginaceae* [8, 10]. Pistil-expressed

Table 3 Primers used for qRT-PCR validation

Unigenes	KEEG Annotation	Gene	Forward 5'–3'	Reverse 5'–3'
CL12551Contig1	Apoptosis	Serine/threonine-protein kinase	TATCCCTTTTCCGATCTTCGCTAT	CAAAGATGAGTTGCTTTTCGTGTTG
CL23964Contig1	Calcium signaling pathway	calcineurin B-like protein	AAATTTGCATATCTGCCTGTGTC	ATGTA AACATCCAAAACCCAGTC
CL32645Contig1	Flavonoid biosynthesis	ANR	AGTATGGCTTTTGTGCTTTGATTGA	TAGAGGTGTCAAGGTTTCAGTTTCA
CL28991Contig1	Flavonoid biosynthesis	CYP75A(F3'5'H)	TTGTAAGTATGGGAGTTTGGGTAGG	CGACACATCATCAAGCGTAATAGAG
CL26013Contig1	Flavonoid biosynthesis	LDOX	AGTTGGCTAATAATGCTAGTGGTCA	TTTTCTAGTCGGCCTTCTTAGTC
CL20835Contig1	negative regulation of programmed cell death	Probable WRKY 40	ATTGACTTGTGCGAAATGTCTGTT	CAATGTTAACCCACTTCCACTACAC
CL1Contig2502	Plant-pathogen interaction	caffeoyl-CoA O-methyltransferase	TCACAAGAACCAGACACAAACATTC	TAAATGGGCACAAGGGTTATGTTTC
CL41260Contig1	Plant-pathogen interaction	CPK	GATTCCTAAACATTTCCAAGCCACA	CTTTAATGTTGGACGGTGAGAAA
CL25650Contig1	Plant-pathogen interaction	PR1	ACCGTTATTTGTACTACTGAACCCCTA	TATGCTAATTCGAGGATGGGTGATT
CL21816Contig1	Plant-pathogen interaction	RPS2	CCAATGGGACCTCTGAACCTATTTTG	TGCTTAAATTCCTTTCAACGAAGA
CL2609Contig1	Plant-pathogen interaction	CALM	TGAAATCTATCATTCCATCCCGT	GAAGGGAGCTTTTGATGTGTTGAT
CL1Contig5289	ubiquitin mediated proteolysis	Skp1	TGGGTTCCAATGGTATTGTTTGAAG	CGAGTGGATTATCGTTCAGTTGATG
CL1Contig1054	ubiquitin mediated proteolysis	Cullin-1	ATATGTGTGGTAACCCATTTGTGTC	AATCCCCGTA AACAGTTCATAGA
CL25362Contig1	Response to auxin	Protein TIFY 9	ATTGACGATTTTCTACAACGGAACC	TCTCCAGAAGTTGATGTTGATCTGT
CL31783Contig1	Response to salicylic acid	12-oxophytodienoate reductase 11	TCATAACAAGGGTGGGATCTTCTTT	CACTGTATCTTTCATGAAGTGGTCG
CL25983Contig1	-	Ribonuclease, T2 family	CTGCGATAGCCGCAACTCTT	GGAAGTAGCTGTGCTGGTCAA
GE651107	Reference gene	GAPDH	GGAAGCATCATGAACTCAAAGTGAA	ATCCTTCTCATTGACACCCATAACA



S-RNase acts as a type of cytotoxin for self-pollen rejection [52]. It was first cloned from *Nicotiana glauca* [51], then transgenic analyses in *Petunia inflata* prove that the S-RNase is the pistil determinant during the pollen rejection interaction [53]. Recently, S-RNase has been identified in various species, such as *Solanaceae* [51], *Prunus* [54], *Malus* [55], *Pyrus* [56], *Antirrhinum* [57], and *Citrus* [4].

A putative *S-RNase* gene (CL25983Contig1), which had strong homology to *ribonuclease T2* gene, was obtained. A phylogenetic tree, based on the amino acid sequence of CL25983Contig1 and S-RNases from other species (Fig. 10), revealed 4 main groups. S-RNases from *Malus* and *Pyrus* were clustered in group I. The sequence from *Coffea canephora* was in group II. CL25983Contig1 and other S-RNases from *Petunia*, *Solanum*, *Nicotiana*, *Medicago*, *Antirrhinum* and *Citrus* were clustered in group III. All of the sequences from *Prunus* were clustered together in group IV. CL25983Contig1 was most closely related to S-RNases from *Citrus reticulata*, *Antirrhinum hispanicum* and *Medicago truncatulata*.

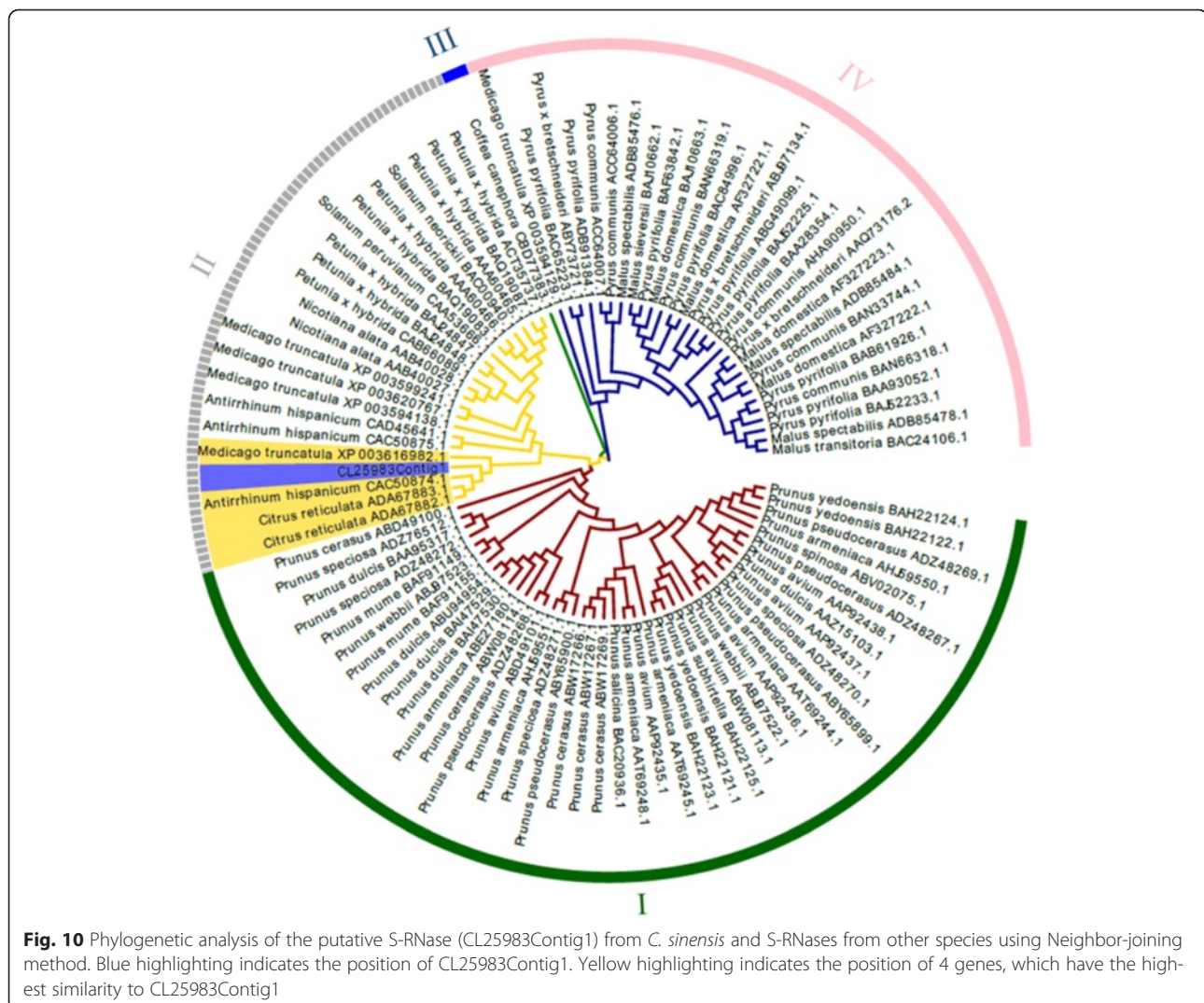
qRT-PCR of CL25983Contig1 in different tissues of tea (Fig. 11) confirmed that this gene was expressed at much higher levels in styles than other tissues such as filaments, leaves, petals and pollens. Moreover, the expression level of CL25983Contig1 increased at 24 h after self-pollination and was 7.45 times higher than that

of cross-pollination (Fig. 12). Interestingly, the pollen tube growth in SP was hindered at 24 h. This suggests that CL25983Contig1 plays an important role in the SI reaction.

Recently, LSI has been demonstrated in many different species; however, the molecular mechanism for LSI is not well understood [6, 13]. LSI is defined based on the location of self-pollen inhibition rather than the molecular mechanism [12]. LSI can be regulated in different ways, through gametophytic or sporophytic control, either independently or acting together [13, 58]. For the pollen tube growth from a self-pollination that was arrested in the ovary, self-incompatibility in *C. sinensis* was assumed to occur via LSI [6, 23, 24]. Because growth of pollen tubes from self-pollination was halted in the style to a certain extent, and several SCF components-encoding genes and a putative *S-RNase* were identified, LSI in tea is likely under gametophytic control.

Conclusions

Transcriptome analysis of styles after cross- and self-pollination in tea has identified a set of candidate genes involved in self-incompatibility. High levels of expression of several SCF components-encoding genes and a putative *S-RNase* gene suggest that LSI in *C. sinensis* might be under gametophytic control. Our study offers novel



insights into the molecular mechanism behind SI in *C. sinensis*. We believe that this RNA-seq data will be useful for breeding and genomics research in *C. sinensis* as well as other plants in the Theaceae family.

Methods

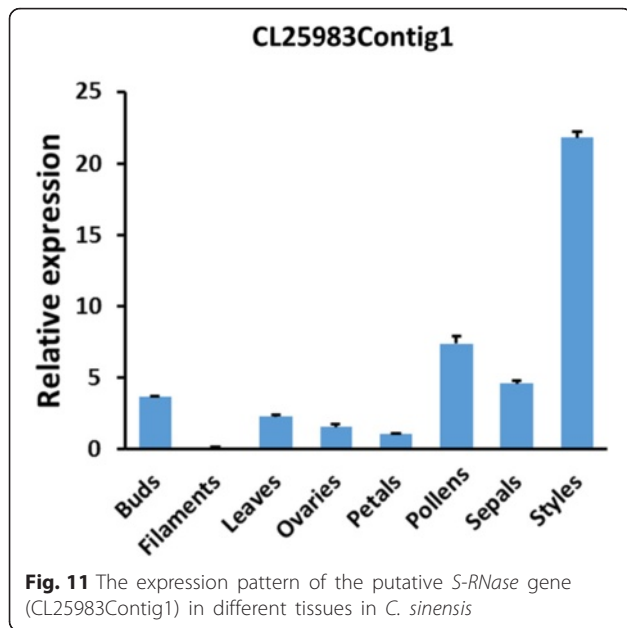
Plant material

Two cultivars of 'Fuding Dabaicha' and 'Zhongcha 108', grown in the China National Germplasm Hangzhou Tea Repository, were used in this study. 'Fuding Dabaicha' is used in many tea-breeding programs in China and more than 18 % of national elite cultivars are derived from it [51]. While 'Zhongcha 108' is a radiation-induced cultivar selected by the Tea Research Institute Chinese Academy of Agricultural Sciences. The reproductive organs and seed-setting rate of these two cultivars are normal. The following tissues were collected from 'Fuding Dabaicha': buds, leaves, filaments, petals, pollens, sepals, unpollinated styles

and ovaries with 3 biological replicates. The samples were frozen immediately in liquid nitrogen and stored at -80°C .

Pollination treatment

Pollens of 'Fuding Dabaicha' and 'Zhongcha 108' were periodically collected from "balloon" stage flowers by placing them in a desiccator at room temperature for 8 h. Pollination was performed from 9:00-11:00 am and 1:00-3:00 pm on sunny days in November. Pollination combinations included self-pollination (SP) of 'Fuding Dabaicha' \times 'Fuding Dabaicha' and cross-pollination (CP) of 'Fuding Dabaicha' \times 'Zhongcha 108'. Flowers in the "balloon" stage were bagged after emasculation and self- or cross-pollinated. The styles were harvested at different intervals (0 h, 2 h, 6 h, 12 h, 24 h, 48 h, 72 h, 96 h and 120 h) after pollination. Therefore, the number of self-pollinated samples ranged from SP0 (0 h after pollination) to SP120 (120 h after pollination). Similarly, the number of cross-pollinated samples ranged from CP0 to CP120.



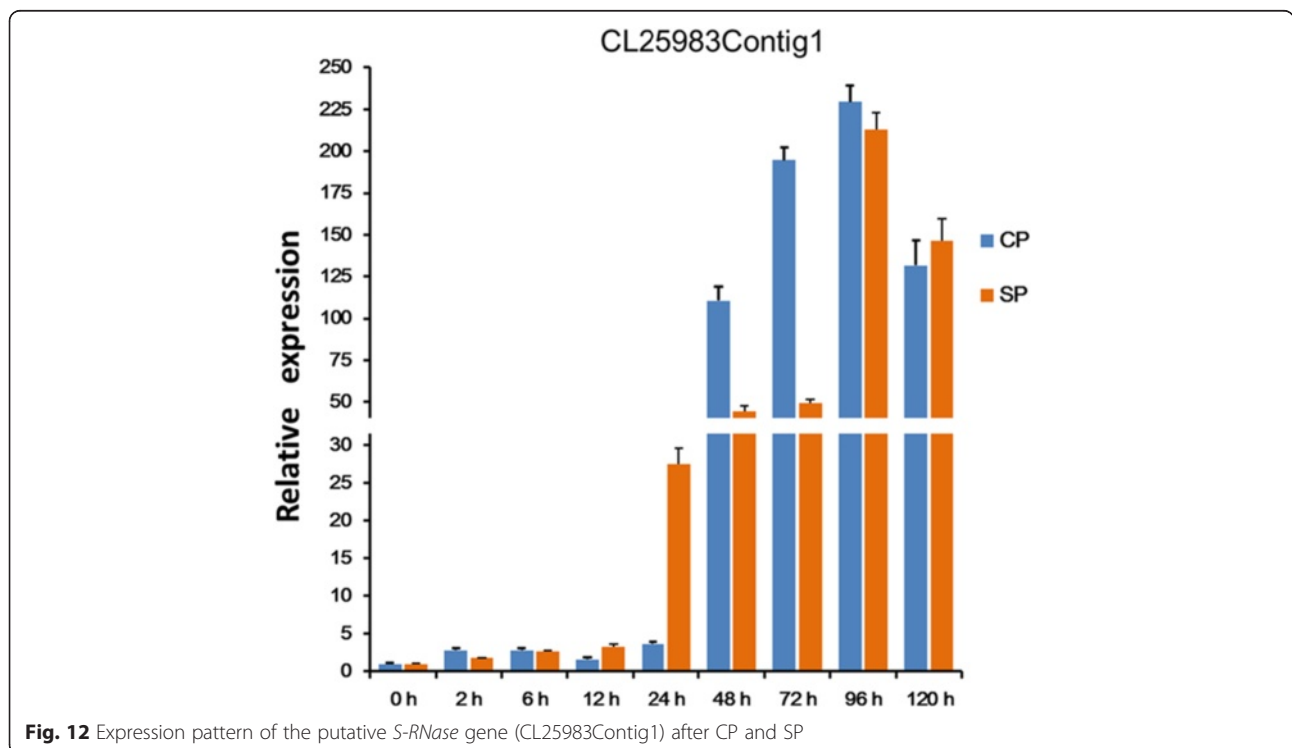
After harvesting, half of the styles of each sample were fixed in FAA (formalin:acetic acid:alcohol 5:5:90 v/v) for 3 h. The remaining styles were divided into two parts, one for RNA-seq and another for qRT-PCR with three biological replicates. Finally, the materials were frozen in liquid nitrogen and stored at -80°C .

Observation of pollen tube growth

After removing the styles from FAA, the styles were macerated with 3 M NaOH for 3 h. Then, the styles were split along the vertical axis into 3 sections, and stained by 1 % aniline blue for 3 h. Finally, the pollen tubes were observed using a Nikon Eclipse 80i fluorescence microscope (Nikon Instech Co. Ltd., Kawasaki, Japan).

RNA extraction, library construction and sequencing

Total RNAs were extracted from self- and cross-pollinated styles using an RNAPrep pure Plant Kit (Tiangen, Beijing, China). The quality of the total RNA was confirmed by electrophoresis through a 1 % agarose gel followed by viewing, and using a NanoDrop 2000 (Thermo Scientific, DE, USA). RNAs from 6 samples (SP24, SP48, SP72, CP24, CP48, and CP72) were used for RNA-seq. The mRNA was isolated from 6 μg total RNA using the Truseq RNASample Prep Kit (Illumina, San Diego, CA, USA). Next, the mRNA was mixed with fragmentation buffer for mRNA fragmentation. After the short fragment, mRNAs were used as template for the first-strand cDNA synthesis using random hexamer-primers, the second-strand cDNA was synthesized and then purified using a SuperScript Double-Stranded cDNA Synthesis Kit (Invitrogen, Carlsbad, CA, USA) and PCR extraction kit (Takara Bio, Otsu, Japan), respectively. The cDNA library was then created following end-repair, polyA addition, adaptor ligation and PCR amplification. After that, cDNA libraries were evaluated using an



Agilent 2100 Bioanalyzer (Agilent Technologies, Palo Alto, Calif.) and sequenced on an Illumina HiSeq™ 2000.

De novo assembly and annotation

Raw RNA-seq data were preprocessed by first removing adaptor and low quality sequences ($Q < 20$ or less than 35 bp) and the qualified reads were then assembled into non-redundant transcripts by Trinity [59] and TGICL [60]. All non-redundant transcripts were annotated to the NR, SWISSPROT, KOG and KEGG databases by blastx using a threshold of $1e^{-5}$. GO term distribution for each transcript was carried out using Blast2GO software [61].

Differential gene expression analysis

The expression of each gene was estimated by FPKM, which was calculated based on the universal reads from 6 separate libraries [62]. Seven groups including CP24 vs. CP48, CP48 vs. CP72, CP24 vs. SP24, CP48 vs. SP48, CP72 vs. SP72, SP24 vs. SP48 and SP48 vs. SP72 were compared. To identify differentially expressed genes, differential expression analysis of the comparisons was performed using a DESeq program (<http://bioconductor.org/packages/release/bioc/html/DESeq.html>). *P*-values related to the analysis of differentially expressed genes were adjusted for multiple testing by the Benjamini-Hochberg false discovery rate (FDR) method [63]. For each comparison, we extracted those unigenes with a criteria of FDR-adjusted *P*-value ≤ 0.05 and $|\log_2\text{Ratio}| > 1$. Furthermore, the differentially expressed unigenes were annotated to the KEGG database using blastx. GO term distribution was performed by a Blast2go software using an FDR-adjusted *P*-value ≤ 0.05 as the cutoff. The genes, which expressed differentially in the comparison of CP24 vs. SP24, CP48 vs. SP48 and CP72 vs. SP72, were used to screen candidate genes for SI.

Comparison of differential gene expression patterns between CP and SP

A STEM software (Carnegie Mellon University, USA) was employed to analyze different patterns of gene expression between CP and SP. Differentially expressed genes in the comparisons of CP24 vs. CP48 and CP48 vs. CP72 were used to cluster changing patterns of CP treatments (Additional file 3). Similarly, differentially expressed genes in the comparison of SP24 vs. SP48 and SP48 vs. SP72 were used to cluster changing patterns of SP treatments (Additional file 3). GO-term analysis was utilized to determine the potential functions of times series genes. GO term with a FDR-adjusted *P*-values ≤ 0.05 was considered to be significantly enriched. The heat map was generated using MeV software (www.tm4.org/mev.html). The multiple alignments of amino acid sequences were constructed using DNAMAN software (www.lynnon.com).

Validation by quantitative real-time PCR (qRT-PCR)

Fifteen differentially expressed transcripts were selected for validation of sequencing data using qRT-PCR. Specific primers were designed by Primer 5 software (Premier Biosoft International, Palo Alto, CA). Total RNA was extracted using an RNAPrep pure Plant Kit (Tiangen, Beijing, China) from the styles. One microgram of total RNA was used to synthesize cDNA using a PrimeScript® 1st Strand cDNA Synthesis Kit (Takara, Dalian, China). Then, qRT-PCR was performed on the ABI 7500 Real-Time PCR System (Applied Biosystems) using a PrimeScript™ RT reagent qPCR Kit (Takara, Dalian, China). A *GADPH* (GE651107) gene was utilized as the reference gene. The real time PCR program was as follows: 95 °C for 15 s, 40 cycles at 95 °C for 5 s, 60 °C for 34 s. Each reaction was repeated three times for biological and technical replicates, respectively. The relative quantitation of the gene expression was calculated using the $2^{-\Delta\Delta C_t}$ method [64].

Expression analysis of a putative S-RNase gene

The amino acid sequence of CL25983Contig1 was predicted using a DNASTAR program Editseq option (DNASTAR, Inc., Madison, Wis.). A phylogenetic tree was constructed using the amino acid sequence deduced from CL25983Contig1 and 93 S-RNases from other species by a Neighbor-joining method by using MEGA 5.2 (www.megasoftware.net). Total RNA was extracted from 8 different tissues. The expression pattern of CL25983Contig1 was examined using qRT-PCR with a reference gene *GADPH*. Furthermore, the expression profiling of CL25983Contig1 was detected in both two pollination treatments from 0 h to 120 h after pollination. Each reaction was performed with three biological replicates and three technical replicates.

Availability of supporting data

Sequence data of 6 samples have been deposited in the NCBI SRA database (SRR3290042, SRR3290055, SRR3290062, SRR3290078, SRR3290084 and SRR3290124).

Additional files

Additional file 1: The species distribution of all of the unigenes. (TIF 3926 kb)

Additional file 2: Gene Ontology terms of all of the unigenes. (TIF 9114 kb)

Additional file 3: Differentially expressed genes between cross- and self-pollination samples. (XLSX 1339 kb)

Additional file 4: Temporal expression of genes in cross- and self-pollination samples. (XLSX 1737 kb)

Abbreviations

SP: self-pollination; CP: cross-pollination; FPKM: fragments per kb per million mapped reads; SSI: sporophytic self-incompatibility; SRK: S-receptor kinase; SCR: S-locus cysteine-rich protein; GSI: gametophytic self-incompatibility; SLF/SFB: S-locus F-box protein; PCD: programmed cell death; OSI: ovarian self-

incompatibility; LSI: late-acting self-incompatibility; NGS: next generation sequencing; *C. sinensis*: *Camellia sinensis*; PR-1: pathogenesis-related-1 protein; NAA: 1-naphthaleneacetic acid; SCF: Skp-1-Cullin1-F-box-Rbx1 complex; Skp-1: S-phase kinase-associated protein 1; Rbx1: RING-box protein 1; CUL1: Cullin-1; CDPK: calcium-dependent protein kinase; CaM: calmodulin protein; CML: calmodulin-like protein; CBL: calcineurin B-like protein; STEM: short time-series expression miner software; ROS: reactive oxygen species; SA: salicylic acid; qRT-PCR: Quantitative real-time PCR; KOG: clusters of orthologous groups for eukaryotic complete genomes; NR: NCBI non-redundant protein; KOG: clusters of orthologous groups for eukaryotic complete genomes; KEGG: Kyoto encyclopedia of genes and genomes; Swiss-Prot: Swiss-Prot protein database; GO: gene ontology; NCBI: National Center for Biotechnology Information; RNA-Seq: RNA sequencing; FDR: false-discovery rate.

Competing interests

The authors declare that they have no competing interests.

Authors' contributions

HC and CCZ conceived and designed the study. CCZ and LY Wang drafted the manuscript. HC and DJN critically reviewed the manuscript. CCZ, LY Wu, HLL and FZ collected and prepared the samples for pollen tube growth observation and RNA sequencing. LY Wang, KW and CCZ analyzed the data. All authors read and approved the final manuscript.

Acknowledgments

The study was supported by the Modern Agro-industry Technology Research System (nycyt-x-23) and The Major Science and Technology Special Project of variety breeding of Zhejiang Province (2012C2905-8).

Received: 28 October 2015 Accepted: 6 May 2016

Published online: 17 May 2016

References

- Wheeler MJ, de Graaf BHJ, Hadjiosif N, Poulter NS, Osman K, Perry RM, et al. Identification of the pollen self-incompatibility determinant in *Papaver rhoeas*. *Nature*. 2009;459:992–5.
- Franklin-Tong VE, Ride JP, Franklin FCH. Recombinant stigmatic self-incompatibility (S-) protein elicits a Ca²⁺ transient in pollen of *Papaver rhoeas*. *Plant J*. 1995;8:299–307.
- Zhou Q, Jia J, Huang X, Yan X, Cheng L, Chen S, et al. The large-scale investigation of gene expression in *Leymus chinensis* stigmas provides a valuable resource for understanding the mechanisms of poaceae self-incompatibility. *BMC Genomics*. 2014;15:399.
- Zhang S, Ding F, He X, Luo C, Huang G, Hu Y. Characterization of the 'Xiangshui' lemon transcriptome by de novo assembly to discover genes associated with self-incompatibility. *Mol Genet Genomics*. 2015;290:365–75.
- Liao T, Yuan DY, Zou F, Gao C, Yang Y, Zhang L, et al. Self-Sterility in *Camellia oleifera* May Be Due to the Prezygotic Late-Acting Self-Incompatibility. *PLoS One*. 2014;9:e99639.
- Gibbs PE. Late-acting self-incompatibility - the pariah breeding system in flowering plants. *New Phytol*. 2014;203:717–34.
- Wang L, Peng H, Ge T, Liu T, Hou X, Li Y. Identification of differentially accumulating pistil proteins associated with self-incompatibility of non-heading Chinese cabbage. *Plant Biol*. 2014;16:49–57.
- Murfett J, Atherton TL, Mou B, Gassert CS, McClure BA. S-RNase expressed in transgenic *Nicotiana glauca* causes S-allele-specific pollen rejection. *Nature*. 1994;367:563–6.
- Sijacic P, Wang X, Skirpan AL, et al. Identification of the pollen determinant of S-RNase-mediated self-incompatibility. *Nature*. 2004;429:302–5.
- McClure B. New views of S-RNase-based self-incompatibility. *Curr Opin Plant Biol*. 2006;9:639–46.
- Thomas SG, Franklin-Tong VE. Self-incompatibility triggers programmed cell death in *Papaver* pollen. *Nature*. 2004;429:305–9.
- LaDoux T, Friar EA. Late-Acting Self-Incompatibility in *Ipomopsis tenuifolia* (Gray) V. Grant (Polemoniaceae). *Int J Plant Sci*. 2006;167:463–71.
- Allen AM, Hiscock SJ. Evolution and phylogeny of self-incompatibility systems in angiosperms. In: Franklin-Tong VE, editor. *Self-incompatibility in flowering plants—evolution, diversity and mechanisms*. Berlin: Springer; 2008. p. 73–100.
- Caruso M, Merelo P, Distefano G, La Malfa S, Piero ARL, Tadeo F, et al. Comparative transcriptome analysis of styler canal cells identifies novel candidate genes implicated in the self-incompatibility response of *Citrus clementina*. *BMC Plant Biol*. 2012;12:20.
- Luna I, Ochoterena H. Phylogenetic relationships of the genera of Theaceae based on morphology. *Cladistics*. 2004;20:223–70.
- Tan LQ, Wang LY, Wei K, Zhang CC, Wu LY, Qi QN, et al. Floral transcriptome sequencing for SSR marker development and linkage map construction in the tea plant (*Camellia sinensis*). *Plos One*. 2013;8(11):e81611.
- Ma JQ, Zhou YH, Ma CL, Yao MZ, Jin JQ, Wang XC, et al. Identification and characterization of 74 novel polymorphic EST-SSR markers in the tea plant, *Camellia sinensis* (Theaceae). *Am J Bot*. 2010;97:e153–6.
- Jaillon O, Aury JM, Noel B, Policriti A, Clepet C, Casagrande A, et al. The grapevine genome sequence suggests ancestral hexaploidization in major angiosperm phyla. *Nature*. 2007;449:463–7.
- Wang XC, Zhao QY, Ma CL, Zhang ZH, Cao HL, Kong YM, et al. Global transcriptome profiles of *Camellia sinensis* during cold acclimation. *BMC Genomics*. 2013;14:415.
- Shi CY, Yang H, Wei CL, Yu O, Zhang ZZ, Jiang CJ, et al. Deep sequencing of the *Camellia sinensis* transcriptome revealed candidate genes for major metabolic pathways of tea-specific compounds. *BMC Genomics*. 2011;12:131.
- Tomimoto Y, Ikehashi H, Kakeda K, Koyama Y. A pistil-specific PR-1 like protein of *Camellia*, its expression, sequence and genealogical position. *Breeding Sci*. 1999;49:97–104.
- Wang Y, Jiang CJ, Zhang HY. Observation on the Self-incompatibility of Pollen Tubes in Self-pollination of Tea Plant in Style in vivo. *Tea Science*. 2008;28:429–35.
- Wachira FN, Kamunya SK. Pseudo-self-incompatibility in some tea clones (*Camellia sinensis* (L) O Kuntze). *J Hort Sci Biotech*. 2005;80:716–20.
- Chen X, Hao S, Wang L, Fang W, Wang Y, Li X. Late-acting self-incompatibility in tea plant (*Camellia sinensis*). *Biologia*. 2012;67:347–51.
- Wang YH, Li XC, Zhu-Ge Q, Jiang X, Wang WD, Fang WP, et al. Nitric oxide participates in cold-inhibited *Camellia sinensis* pollen germination and tube growth partly via cGMP in vitro. *PLoS One*. 2012;7:e52436.
- Chen X, Liu T, Hao S, Fang W, Wang Y, Li X. Differential gene expression analysis of self-incompatible lines in tea by cDNA-AFLP. *Afr J Biotechnol*. 2011;10:10906–13.
- Baker RP, Hasenstein KH, Zavada MS. Hormonal changes after compatible and incompatible pollination in *Theobroma cacao* L. *HortScience*. 1997;32:1231–4.
- Hasenstein KH, Zavada MS. Auxin modification of the incompatibility response in *Theobroma cacao*. *Physiol Plantarum*. 2001;112:113–8.
- Zhao P, Zhang L, Zhao L. Dissection of the style's response to pollination using transcriptome profiling in self-compatible (*Solanum pimpinellifolium*) and self-incompatible (*Solanum chilense*) tomato species. *BMC Plant Biol*. 2015;15:119.
- Steinhorst L, Kudla J. Calcium—a central regulator of pollen germination and tube growth. *BBA-Mol Cell Res*. 1833;2013:1573–81.
- Brewbaker JL, Kwack BH. The essential role of calcium ion in pollen germination and pollen tube growth. *Am J Bot*. 1963;50:859–65.
- Miao HX, Ye ZX, Qin YH, Hua GB. Identification of differentially expressed genes in 72 h styles from self-incompatible *Citrus reticulata*. *Scientia Horticulturae*. 2013;161:278–85.
- Hua ZH, Kao TH. Identification of major lysine residues of S3-RNase of *Petunia inflata* involved in ubiquitin-26S proteasome-mediated degradation in vitro. *Plant J*. 2008;54:1094–104.
- Zhang Y, Zhao Z, Xue Y. Roles of proteolysis in plant self-incompatibility. *Annual Rev Plant Biol*. 2009;60:21–42.
- Zhao L, Huang J, Zhao Z, Li Q, Sims TL, Xue Y. The Skp1-like protein SSK1 is required for cross-pollen compatibility in S-RNase-based self-incompatibility. *Plant J*. 2010;62:52–63.
- Matsumoto D, Yamane H, Abe K, Tao R. Identification of a Skp1-like protein interacting with SFB, the pollen S determinant of the gametophytic self-incompatibility in *Prunus*. *Plant Physiol*. 2012;159:1252–62.
- Li S, Šamaj J, Franklin-Tong VE. A mitogen-activated protein kinase signals to programmed cell death induced by self-incompatibility in *Papaver* pollen. *Plant Physiol*. 2007;145:236–45.
- Hua Z, Kao TH. Identification and characterization of components of a putative *Petunia* S-locus F-box-containing E3 ligase complex involved in S-RNase-based self-incompatibility. *Plant Cell*. 2006;18:2531–53.

39. Hiscock SJ, Allen AM. Diverse cell signalling pathways regulate pollen-stigma interactions: the search for consensus. *New Phytol.* 2008;179:286–317.
40. Kao T, Tsukamoto T. The molecular and genetic bases of S-RNase-based self-incompatibility. *Plant Cell.* 2004;16 suppl 1:72–83.
41. Yoon GM, Dowd PE, Gilroy S, McCubbin AG. Calcium-dependent protein kinase isoforms in *Petunia* have distinct functions in pollen tube growth, including regulating polarity. *Plant Cell.* 2006;18:867–78.
42. Zhou L, Fu Y, Yang Z. A genome-wide functional characterization of Arabidopsis regulatory calcium sensors in pollen tubes. *J Integr Plant Biol.* 2009;51:751–61.
43. Potocky M, Jones MA, Bezdova R, Smirnov N, Zarsky V. Reactive oxygen species produced by NADPH oxidase are involved in pollen tube growth. *New Phytol.* 2007;174:742–51.
44. Wang CL, Wu J, Xu GH, Gao YB, Chen G, Wu JY, et al. S-RNase disrupts tip-localized reactive oxygen species and induces nuclear DNA degradation in incompatible pollen tubes of *Pyrus pyrifolia*. *J Cell Sci.* 2010;123:4301–9.
45. Wilkins KA, Bancroft J, Bosch M, Ings J, Smirnov N, Franklin-Tong VE. Reactive oxygen species and nitric oxide mediate actin reorganization and programmed cell death in the self-incompatibility response of papaver. *Plant Physiol.* 2011;156:404–16.
46. Turrens JF. Mitochondrial formation of reactive oxygen species. *J Physiol.* 2003;552:335–44.
47. Neog B, Yadav RNS, Singh ID. Peroxidase, polyphenol oxidase and acid phosphatase activities in the stigma-style tissue of *Camellia sinensis* (L) O. Kuntze following compatible and incompatible pollination. *J Indian Inst Sci.* 2004;84:47–52.
48. Fernandez-Perez F, Pomar F, Pedreño MA, Novo-Uzal E. The suppression of *AtPrx52* affects fibers but not xylem lignification in Arabidopsis by altering the proportion of syringyl units. *Physiologia Plantarum.* 2015;154:395–406.
49. Torres MA, Jones JDG, Dangl JL. Reactive oxygen species signaling in response to pathogens. *Plant Physiol.* 2006;141:373–8.
50. O'Brien M, Kapfer C, Major G, Laurin M, Bertrand C, Kondo K, et al. Molecular analysis of the stylar-expressed *Solanum chacoense* small asparagine-rich protein family related to the HT modifier of gametophytic self-incompatibility in *Nicotiana*. *Plant J.* 2002;32:985–96.
51. Anderson MA, Cornish EC, Mau S-L, Williams EG, Hoggart R, Atkinson A, et al. Cloning of cDNA for a stylar glycoprotein associated with expression of self-incompatibility in *Nicotiana glauca*. *Nature.* 1986;321:38–44.
52. Yu J, Huang H, Yao M, Yang YJ. Analysis of Genetic Diversity and Relationship of Half-sib Tea Cultivars Related to Fuding Dabai and Yunnan Daye Using EST-SSR Markers. *J Tea Sci.* 2010;30:184–90.
53. Lee HS, Huang S, Kao TH. S proteins control rejection of incompatible pollen in *Petunia inflata*. *Nature.* 1994;367:560–3.
54. Ushijima K, Sassa H, Tao R, Yamane H, Dandekar AM, Gradziel TM, et al. Cloning and characterization of cDNAs encoding S-RNases from almond (*Prunus dulcis*): primary structural features and sequence diversity of the S-RNases in Rosaceae. *Mol Gen Genet.* 1998;260:261–8.
55. Broothaerts W, Janssens GA, Proost P, Broekaert WF. cDNA cloning and molecular analysis of two self-incompatibility alleles from apple. *Plant Mol Biol.* 1995;27:499–511.
56. Castillo C, Takasaki T, Saito T, Norioka S, Nakanishi T. Cloning of the S8-RNase (S8-allele) of Japanese Pear (*Pyrus pyrifolia* Nakai). *Plant Biotechnol J.* 2002;19:1–6.
57. Xue Y, Carpenter R, Dickinson HG, Coen ES. Origin of allelic diversity in *Antirrhinum* S locus RNases. *Plant Cell.* 1996;8:805–14.
58. de MF Suassuna T, Bruckner C, de Carvalho C, Borém A. Self-incompatibility in passionfruit: evidence of gametophytic-sporophytic control. *Theor Appl Genet.* 2003;106:298–302.
59. Grabherr MG, Haas BJ, Yassour M, Levin JZ, Thompson DA, Amit I, et al. Trinity: reconstructing a full-length transcriptome without a genome from RNA-Seq data. *Nature biotechnol.* 2011;29:644–52.
60. Pertea G, Huang X, Liang F, Antonescu V, Sultana R, Karamycheva S, et al. TIGR Gene Indices clustering tools (TGICL): a software system for fast clustering of large EST datasets. *Bioinformatics.* 2003;19:651–2.
61. Conesa A, Terol J, Talón M, Robles M. Blast2GO: a universal tool for annotation, visualization and analysis in functional genomics research. *Bioinformatics.* 2005;21:3674–6.
62. Mortazavi A, Schaeffer L, Wold B. Mapping and quantifying mammalian transcriptomes by RNA-Seq. *Nat Methods.* 2008;5:621–8.
63. Benjamini Y, Hochberg Y. Controlling the false discovery rate: a practical and powerful approach to multiple testing. *Journal of the Royal Statistical Society. Series B (Methodological).* 1995;57:289–300.
64. Livaka KJ, Schmittgen TD. Analysis of relative gene expression data using real-time quantitative PCR and the $2^{-\Delta\Delta CT}$ method. *Methods.* 2001;25:402–8.

Submit your next manuscript to BioMed Central and we will help you at every step:

- We accept pre-submission inquiries
- Our selector tool helps you to find the most relevant journal
- We provide round the clock customer support
- Convenient online submission
- Thorough peer review
- Inclusion in PubMed and all major indexing services
- Maximum visibility for your research

Submit your manuscript at
www.biomedcentral.com/submit

